DEPARTMENT OF MATHEMATICS
UNIVERSITY OF NIJMEGEN The Netherlands

BARRIER VARIATIONAL GENERATION OF QUASI-ISOMETRIC GRIDS

V.A. Garanzha

Report No. 0007 (March 2000)

DEPARTMENT OF MATHEMATICS
UNIVERSITY OF NIJMEGEN
Toernooiveld
6525 ED Nijmegen
The Netherlands

Barrier variational generation of quasi-isometric grids

V.A. Garanzha[1]

Abstract

The grid generation method based on the minimization of the discrete barrier functional with feasible set consisting of quasi-isometric grids is suggested. The deviation from isometry for given grid connectivity and fixed boundary nodes is minimized via the contraction of the feasible set into small vicinity of the optimal grid. Formulation of functional with given metrics in both physical and logical spaces allows to consider the adaptive grid generation in terms of quasi-isometric grids and cover many practical applications. The fast and reliable procedure for finding feasible solution based on the penalty-like reformulation of barrier functional and the continuation technique is described. The relations between different barrier approximations to quasi-isometric functional in 2-D and 3-D cases are investigated. Numerical experiments have confirmed that the suggested functional allows to obtain high quality grids.

1 Introduction.

A class of the most reliable methods for grid generation in complicated domains is based on variational approaches. We consider, in particular, methods based on or derived from the quasi-conformal mappings [2], [3] and on harmonic mappings [1], [4], [6], [9]. In this approach the computational grids are constructed via the minimization of a discrete counterpart of the Dirichlet functional and its generalizations.

Typically variational grid generation should be considered as a constrained minimization problem since it assumes the maximization of some grid quality measure subject to the grid non-degeneracy constraint.

Let the computational grid in the n-dimensional space $\{x_1, \ldots, x_n\}$ be represented by the vector

$$\mathbf{R} = \begin{pmatrix} \mathbf{X}^1 \\ \ldots \\ \mathbf{X}^n \end{pmatrix}, \ \mathbf{X}^i \in I\!R^{N_v},$$

where $\mathbf{X}^i$ denotes the vector consisting of all x^i-coordinates of the grid nodes and N_v is the total number of the grid nodes. We seek $\mathbf{R}$ as a mininum of the functional $\mathcal{I}^h(\mathbf{R})$ which is defined on the open feasible set $\mathcal{F}$ consisting of nondegenerate grids with given connectivity and fixed boundary nodes. We consider only such functionals

[1]Computing Center RAS, Moscow, e-mail: garan@ccas.ru.
The support of this research via the INTAS-RFBR grant 0095-98 is gratefully aknowledged.

$\mathcal{I}^h(\mathbf{R})$ which are at least twice differentiable, positive and bounded functions of $\mathbf{R}$ in any connected subset of feasible set and

$$\lim_{\mathbf{R}\in\mathcal{F},\ \operatorname{dist}(\mathbf{R},\partial\mathcal{F})\to 0} \mathcal{I}^h(\mathbf{R}) = +\infty. \tag{1}$$

The presence of the barrier of the "first kind" (1) guarantees that the barrier functional has at least one stationary point inside the feasible set. In [8], [9] it was shown that some discrete approximations to the generalized Dirichlet functional have a barrier on the boundary of the set of grids consisting of convex quadrilateral cells.

The gradient of the barrier functional should possess the barrier property as well

$$\lim_{\mathbf{R}\in\mathcal{F},\ \operatorname{dist}(\mathbf{R},\partial\mathcal{F})\to 0} \|\nabla\mathcal{I}^h(\mathbf{R})\| = +\infty,$$

where $\|\cdot\|$ denotes, for example, the 2-norm in $\mathbb{R}^{n\mathbf{N}_v}$. The presence of this barrier of the "second kind" guarantees the existence of the constant c such that $\operatorname{dist}(\mathbf{R}_s, \partial\mathcal{F}) \geq c > 0$, where $\mathbf{R}_s$ is a stationary point of the functional $\mathcal{I}^h(\mathbf{R})$. The simple example of the 1-D function

$$f(x) = \frac{1}{x}(2 + \sin(\frac{1}{x})), \quad \mathcal{F} = \{x, x > 0\},$$

where stationary points can be found in arbitrary small vicinity of the feasible set boundary $x = 0$ illustrates the importance of the second barrier for nonconvex functionals which are typical in grid generation.

Similar problems arise in mechanics of hyperelasticity, where it is necessary to construct nondegenerate mappings which led to the formulation of the principle of extremal states [14], [19], [18]. It seems that this principle can be identified with the presence of the barrier property for the gradient of the functional. Moreover, in [19] on the continuous level it was shown that this principle is incompatible with convexity of the functional. Hence after discretization it is quite natural to expect that the resulting grid functionals will be nonconvex as well. However demonstrating the existence of a barrier of second kind for discretized grid functionals is a difficult and not a totally resolved problem.

The practical solution to the problem of constructing feasible solutions for barrier functionals can be based on the penalized formulation, when the original barrier functional $\mathcal{I}^h(\mathbf{R})$ is replaced by the regularized one $\mathcal{I}^h_\varepsilon(\mathbf{R})$ with the following properties:

$$\lim_{\mathbf{R}\in\mathcal{F},\ \varepsilon\to 0} |\mathcal{I}^h(\mathbf{R}) - \mathcal{I}^h_\varepsilon(\mathbf{R})| = 0, \quad \lim_{\mathbf{R}\notin\mathcal{F},\ \varepsilon\to 0} \mathcal{I}^h_\varepsilon(\mathbf{R}) = +\infty, \tag{2}$$

$$\lim_{\mathbf{R}\notin\mathcal{F},\ \varepsilon\to 0} \|\nabla\mathcal{I}^h_\varepsilon(\mathbf{R})\| = +\infty, \tag{3}$$

and $\mathcal{I}^h_\varepsilon(\mathbf{R})$ is at least twice differentiable everywhere. Typically (2) is relatively easy to prove, while the proof of equality (3) which guarantees that limiting stationary points of penalized functional belong to feasible set can be very difficult.

Recently it became a widespread practice to improve the quality of unstructured grids by applying variational methods in an element-by-element manner. It is done

typically by using the functionals which maximize the quality of the local mapping for each cell of the grid along with the conventional finite element assembly procedure. In the case of regular grid connectivity this approach is equivalent to mapped grid generation methods while being applicable to block-structured and unstructured grid generation.

Various grid quality measures can be used for constructing the functional $\mathcal{I}^h(\mathbf{R})$, see for example, [5], [6], [7], [21]. In the case of quality measure t, "dimensionless" in a sense that $0 \leq t \leq 1$, it is possible to consider the parameterized feasible set $\mathcal{F}(t)$, consisting of grids where the quality of each cell is above a threshold value t. Then $\mathcal{F}(0)$ denotes the set of non-degenerate grids and $\mathcal{F}(1)$ is the grid consisting of "ideal" cells. Typically in barrier grid generation methods [8], [9] and in barrier construction of nondegenerate mappings [14], [19], [18], the barrier is constructed on $\partial\mathcal{F}(0)$. The basic idea of the present work is to construct the barrier on $\partial\mathcal{F}(t)$ and to "contract" it which means to find the grid with the maximum possible quality measure $t = t_{\max}$.

If it is possible to show that

$$\mathcal{F}(t_1) \subset \mathcal{F}(t_2), \quad t_1 > t_2 \quad \text{and} \quad \mathcal{F}(t) = \emptyset, \quad t > 1,$$

then one can expect that for given grid connectivity and fixed boundary nodes there exists $0 < t = t_{\max} \leq 1$, such that

$$\lim_{t \to t_{\max}, t \leq t_{\max}} \operatorname{diam}(\mathcal{F}(t)) = 0,$$

provided that $\mathcal{F}(0)$ is simply-connected. The relations between barriers are shown on Figure 1.

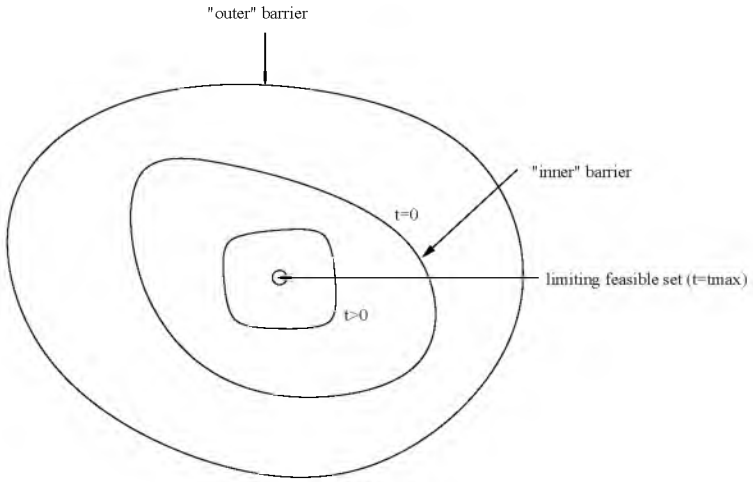

Fig. 1.

However this scenario is too optimistic since one can expect that not the diameter but the measure of the feasible set will tend to 0, or, in particular, that for $t > t_0 \geq 0$ the feasible set $\mathcal{F}(t)$ will become the union of disjoint simply connected domains with

diameters tending to 0. It should be noted that search for global extremum inside connected feasible set does not make much sense, since one of the main requirements for grid generation methods is continuous dependence on input data. As soon as nonuniqueness is detected this requirement is not met and one can consider as a final solution any grid belonging to the vicinity of the set of quasi-solutions which have practically the same quality [17]. It is a known fact that barrier grid functionals can have multiple stationary points [17], however the sufficient conditions guaranteeing uniqueness are still not known.

Summing up, the barrier grid generation method should include the following basic components

(a) variational principle;

(b) barrier approximation to target functional;

(c) procedure for contracting the set of admissible grids;

(d) penalized formulation and the procedure for constructing feasible solution;

(e) efficient minimization technique.

The present paper focuses on items (a)-(d). The minimization procedure is similar to that in [17] but is more complicated and requires a separate paper for full description.

Since our goal is the grid generation and not the construction of the mappings, we will not consider the justification of the functionals, the solvability problems and the regularity of solutions on the continuous level.

2 Variational principle

Our aim is to find the function

$$\mathbf{r} = \mathbf{r}(\xi_1, \ldots, \xi_n), \mathbf{r} = (x_1, \ldots, x_n)^T \tag{4}$$

which is the one-to-one mapping of the regular-shaped domain $\mathcal{D}$ such as unit cube in $\{\xi_1, \ldots, \xi_n\}$ coordinates onto a domain Ω in physical coordinates.. We will consider later the mappings for other types of regular-shaped domains, in particular for tetrahedra in the case $n = 3$.

Let us introduce the following notations

$$\mathbf{g}_i = \frac{\partial \mathbf{r}}{\partial \xi_i}, \quad S = (\mathbf{g}_1, \ldots, \mathbf{g}_n), \quad \mathrm{adj}S = S^{-1} \det S, \quad \mathrm{adj}S^{\mathrm{T}} = (\mathbf{g}^1, \ldots, \mathbf{g}^n),$$

where $\mathbf{g}_i$ are the covariant basis vectors of mapping (4) and S is the Jacobian matrix.

According to the theory of harmonic mappings [13] we start our analysis by seeking (4) as the inverse harmoning mapping or as the solution to the following problem

$$\mathbf{r}(\xi) = \arg\min \int_{\mathcal{D}} \frac{\mathrm{tr}(H^{\mathrm{T}} H \, \mathrm{adj}S \, G^{-1} \, \mathrm{adj}S^{\mathrm{T}})}{(\det G)^{-\frac{1}{2}} \det S} \, d\xi, \tag{5}$$

subject to the constraint

$$\det S > 0,$$

given that the one-to-one mapping of $\partial\mathcal{D}$ onto $\partial\Omega$ is specified. Here $G = G^T > 0$, $G = G(\mathbf{r})$ is the metrics in the physical coordinates, $H = H(\xi)$ and $H^T H > 0$ is the "accompanying" metrics defined in the logical space.

The generic formulation (5) covers several important cases, in particular in the case $H = I$ one obtains the generalized Dirichlet functional

$$\int_{\Omega} \sum_{i=1}^{n} (\nabla \xi_i)^T G^{-1} (\det G)^{\frac{1}{2}} \nabla \xi_i \, dx,$$

which is used in many applications, in particular in those based on the monitoring function concept. Here the dependent and independent variables are interchanged using the assumption that $\det S > 0$.

Another limiting case $G = I$ leads to the functional first used for grid generation by Godunov and Prokopov,

$$\int_{\mathcal{D}} \sum_{i,j=1}^{n} \frac{(\sum_{k=1}^{n} h_{ki} h_{kj}) \mathbf{g}^{i\,\mathrm{T}} \mathbf{g}^{j}}{J} \, d\xi.$$

Let us cast functional (5) in the 2-D case into different form. Using the equality

$$\mathrm{tr}(H^{\mathrm{T}} H \, \mathrm{adj} S \, G^{-1} \, \mathrm{adj} S^{\mathrm{T}}) = \mathrm{tr}(\mathrm{adj} G^{-1} \, S \, \mathrm{adj}(H^{\mathrm{T}} H) \, S^{\mathrm{T}}),$$

which is valid only for 2×2 matrices, we obtain that in the 2-D case

$$\frac{\mathrm{tr}(H^{\mathrm{T}} H \, \mathrm{adj} S \, G^{-1} \, \mathrm{adj} S^{\mathrm{T}})}{(\det G)^{-\frac{1}{2}} \det S} = \frac{(\det H)^2 \, \mathrm{tr}(H^{-\mathrm{T}} S^{\mathrm{T}} G S H^{-1})}{(\det G)^{\frac{1}{2}} \det S}.$$

Introducing the new notation

$$A = H^{-\mathrm{T}} S^{\mathrm{T}}, \tag{6}$$

we obtain that

$$\frac{\mathrm{tr}(H^{\mathrm{T}} H \, \mathrm{adj} S \, G^{-1} \, \mathrm{adj} S^{\mathrm{T}})}{(\det G)^{-\frac{1}{2}} \det S} = \frac{\det H \, \mathrm{tr}(G A^{\mathrm{T}} A)}{(\det G)^{\frac{1}{2}} \det A} = f(A),$$

and functional (5) can be rewritten as follows

$$\int_{\mathcal{D}} f(A) d\xi. \tag{7}$$

The next step is to extend the above functional to the n-dimensional case as the dimensionless ratio of matrix invariants

$$f(A) = \det H \frac{(\frac{1}{n} \mathrm{tr}(G A^{\mathrm{T}} A))^{\frac{n}{2}}}{\det A (\det G)^{\frac{1}{2}}} = \frac{\det H}{\det A} \phi_c, \quad \phi_c = \frac{(\frac{1}{n} \mathrm{tr}(G A^{\mathrm{T}} A))^{\frac{n}{2}}}{(\det G)^{\frac{1}{2}}}. \tag{8}$$

Obviously the above expression is invariant to arbitrary scaling of A hence we add to (8) the "incompressibility" term allowing to control the value of $\det A$.

$$f(A) = \frac{\det H}{\det A}\phi(A), \;\; \phi(A) = (1-\omega_u)\phi_c + \omega_u\phi_u, \;\; \phi_u = \frac{1}{2}\left(\frac{\overline{v}}{(\det G)^{\frac{1}{2}}} + \frac{(\det G)^{\frac{1}{2}}}{\overline{v}}(\det A)^2\right) \tag{9}$$

where

$$\overline{v} = \int_{\mathcal{D}} (\det G)^{\frac{1}{2}} \det S \, d\xi \, / \int_{\mathcal{D}} \det H \, d\xi,$$

and

$$0 < \omega_u < 1.$$

It is useful to analyze the properties of the function $f(A)$ defined by (9). To this end let us consider the auxiliary minimization problem

$$A = \arg\min_{A} f(A). \tag{10}$$

Omitting the derivation details, the solution A to this minimization problem with $\det A > 0$ looks as follows

$$AGA^{\mathrm{T}} = \frac{1}{n}\operatorname{tr}(GA^{\mathrm{T}}A)I, \;\; \det A = \frac{\overline{v}}{(\det G)^{\frac{1}{2}}} \tag{11}$$

Using the definition of A we obtain that equality (11) is equivalent to

$$S^{\mathrm{T}}GS = \overline{v}^{\frac{2}{n}} H^{\mathrm{T}}H, \;\; \det S = \det H \frac{\overline{v}}{(\det G)^{\frac{1}{2}}},$$

or in the component-wise form

$$\sum_{k,p=1}^{n} \frac{\partial x_i}{\partial \xi_k} g_{kp} \frac{\partial x_j}{\partial \xi_p} = \overline{v}^{\frac{2}{n}} \sum_{k=1}^{n} h_{ik}h_{kj}. \tag{12}$$

In (12) g_{kp} are covariant components of the metrics G and $\sum\limits_{k=1}^{n} h_{ik}h_{kj}$ are the $_{ij}$-th covariant components of the metrics $H^{\mathrm{T}}H$. The above equality is in fact the transformation rule for tensors of the second rank which means that G and $H^{\mathrm{T}}H$ are the same tensors up to the prescribed scalar multiplier and functional (8) can be considered as the measure of deviation between these tensors. The fact that the harmonic functional is the measure of deviation between metrics up to an arbirary scaling was first recognized by S.K. Godunov [25]. However adding the incompressibility terms allows to control this scaling in each point. By incompressible mapping one generally assumes mapping which locally conserves the volume, i.e. $\overline{v} = 1$ but without loss of generality it is possible to consider the case $\overline{v} \neq 1$ which corresponds to global scaling.

As a result in the ideal case mapping (4) becomes isometric, i.e., both conformal and incompressible, and

$$(dl_r)^2 = \overline{v}^{\frac{2}{n}} (dl_\xi)^2,$$

where dl_r, dl_ξ are length differentials in Ω and $\mathcal{D}$, respectively, computed in appropriate metrics:

$$|dl_\xi| = |(d\xi_1, \ldots, d\xi_n)H^{\mathrm{T}}|, \quad |dl_r| = |\mathbf{r}^{\mathrm{T}} G d\mathbf{r}|^{\frac{1}{2}}, \quad d\mathbf{r}^{\mathrm{T}} = (d\xi_1, \ldots, d\xi_n)S^{\mathrm{T}}.$$

Obviously this "ideal" isometric minimum can be attained only in some particular cases. The more realistic problem of constructing quasi-isometric mappings was posed by S.K. Godunov [25] and in our notations can be formulated as follows: find the mapping $\mathbf{r}(\xi_1, \ldots, \xi_n)$, such that

$$\gamma \overline{v}^{\frac{2}{n}} (dl_\xi)^2 < (dl_r)^2 < \Gamma \overline{v}^{\frac{2}{n}} (dl_\xi)^2, \Gamma \geq \gamma > 0, \tag{13}$$

and the ratio Γ/γ, i.e. the isometric condition number, is minimal among all mapping satisfying specified boundary conditions. Inequalities (13) can also be written in the following matrix form

$$\gamma^2 \overline{v}^{\frac{2}{n}} I < AGA^{\mathrm{T}} < \Gamma^2 \overline{v}^{\frac{2}{n}} I \quad \text{or} \quad \gamma^2 \overline{v}^{\frac{2}{n}} H^{\mathrm{T}} H < S^{\mathrm{T}} G S < \Gamma^2 \overline{v}^{\frac{2}{n}} H^{\mathrm{T}} H.$$

It is not clear whether the minimum of functional (7), (9) is the quasi-isometric mapping. Hence let us consider other function $f(A)$ with the feasible set consisting of mappings satisfying (13). It is easy to verify that the solution to the minimization problem

$$A = \arg\min_A f(A), \quad f(A) = (1-t) \det H \frac{\phi(A)}{\det A - t\phi(A)},$$

where $0 < t \leq 1$ also can be found from (11), provided that $\det A - t\phi(A) > 0$. Similar transformations are used in nonlinear programming methods [24], and in terms of [24] the above functional is the exact auxiliary function for (10).

Now we are in a position to formulate the final minimization problem

$$\mathbf{r}(\xi) = \arg\min \int_{\mathcal{D}} (1-t) \det H \frac{\phi(A)}{\det A - t\phi(A)} d\xi, \quad A = (\mathbf{a}_1, \ldots, \mathbf{a}_n), \quad \mathbf{a}_i = H^{-T} \nabla_\xi x_i, \tag{14}$$

subject to the constraint

$$\det A - t\phi(A) > 0. \tag{15}$$

Here ∇_ξ denotes the gradient operator in logical coordinates, $\nabla_\xi x_i = (\frac{\partial x_i}{\partial \xi_1}, \ldots, \frac{\partial x_i}{\partial \xi_n})^{\mathrm{T}}$ and $\phi(A)$ is defined by (9).

We will consider also the following modification of (14)

$$\mathbf{r}(\xi) = \arg\min \int_{\mathcal{D}} (1-t) \frac{\psi(H)\phi(A)}{\det A - t\psi(H)\phi(A)} d\xi, \tag{16}$$

where the function $\psi(H)$ is problem dependent. Below we show that (16) can be used, for example, for construction of grids which are orthogonal near boundary.

2.1 Characterization of the feasible set.

Let us prove that the feasible set $\mathcal{F}(t)$ defined by (15) consists of quasi-isometric mappings. In fact (15) means that

$$\frac{\phi_u}{\det A} < c_1 = \frac{1}{\omega_u t}, \quad \frac{\phi_c}{\det A} < c_2 = \frac{1}{(1-\omega_u)t}.$$

Denoting by $V = AGA^{\mathrm{T}}$, we obtain that

$$\frac{(\frac{1}{n}\operatorname{tr} V)^{\frac{n}{2}}}{(\det V)^{\frac{1}{2}}} < c_1, \quad \frac{\overline{v}}{(\det V)^{\frac{1}{2}}} + \frac{(\det V)^{\frac{1}{2}}}{\overline{v}} < 2c_2,$$

which means that

$$(\beta(V))^{\frac{n}{2}} < c_1, \quad c_2 - \sqrt{c_2^2 - 1} < \frac{(\det V)^{\frac{1}{2}}}{\overline{v}} < c_2 + \sqrt{c_2^2 - 1},$$

where

$$\beta(V) = \frac{\frac{1}{n}\operatorname{tr} V}{(\det V)^{\frac{1}{n}}},$$

is the spherical measure or the Kaporin condition number of the matrix V. Using the Kaporin inequality [23]

$$\operatorname{cond}(V) \le \sqrt{(\beta(V))^n} + \sqrt{(\beta(V))^n - 1},$$

which is valid for any symmetric positive definite matrix V, we obtain that

$$c_1 - \sqrt{c_1^2 - 1} < \frac{\lambda_i(V)}{\lambda_j(V)} < c_1 + \sqrt{c_1^2 - 1},$$

where $\lambda_i(V), \lambda_j(V)$ is any pair of eigenvalues of V, and $\operatorname{cond}(V)$ denotes the conventional condition number of the matrix V. As a result we obtain the final estimates for (13):

$$\gamma = \left(c_2 - \sqrt{c_2^2 - 1}\right)^{\frac{1}{n}} \left(c_1 - \sqrt{c_1^2 - 1}\right)^{\frac{n-1}{2n}}, \quad \Gamma = \left(c_2 + \sqrt{c_2^2 - 1}\right)^{\frac{1}{n}} \left(c_1 + \sqrt{c_1^2 - 1}\right)^{\frac{n-1}{2n}}.$$

The obvious drawback of functional (14) is that the estimates for Γ/γ are not sharp, in particular for isometric mapping and $\omega_u = 1/2$ we obtain $\Gamma/\gamma = (2+\sqrt{3})^{\frac{n+1}{n}}$. In principle this problem can be circumvented using, for example, the functional (7) with

$$f(A) = \det H \left((1-\omega_u)\frac{\phi_c}{\det A - t\phi_c} + \omega_u \frac{\phi_u}{\det A - t\phi_u} \right). \tag{17}$$

In this case the feasible set $\mathcal{F}(t)$ is defined as

$$\mathcal{F}(t) = \mathcal{F}_c(t) \cap \mathcal{F}_u(t),$$

where $\mathcal{F}_c(t)$ consists of quasi-conformal mappings, $\mathcal{F}_u(t)$ consists of quasi-incompressible mappings and

$$\frac{\Gamma}{\gamma} = \left(\frac{1}{t} + \sqrt{\frac{1}{t^2} - 1}\right)^{(n+1)/n}$$

However working with two different barriers simultaneously is a very difficult computational task which we intend to avoid here by using only quasi-optimal formulation (14).

Let us denote by $\nabla_a f$ the gradient of a function $f(A)$ with respect to the columns of A

$$\nabla_a^{\mathrm{T}} f = (\frac{\partial}{\partial \mathbf{a}_1^{\mathrm{T}}} f, \ldots, \frac{\partial}{\partial \mathbf{a}_n^{\mathrm{T}}} f).$$

The following simple statement holds: adding any convex function $p = p(\det A)$ to integrand $f(A)$ which defines an elliptic functional results in elliptic functional provided that $\det A > 0$. It follows from equality

$$\nabla_a \nabla_a^{\mathrm{T}} p = p'' \nabla_a (\det A) \nabla_a^{\mathrm{T}} (\det A) + p' \nabla_a \nabla_a^{\mathrm{T}} (\det A),$$

and the fact that the term $\nabla_a \nabla_a^{\mathrm{T}} (\det A)$ makes any contribution only to lower order terms of linearized Euler-Lagrange equations.

Another simple statement is the following: if an integrand $f(A)$ defines an elliptic functional then the transformed integrand $1/(1/f - t)$ leads to elliptic functional as well, provided that $t \geq 0$ and $1 - ft > 0$. This statement is the obvious consequence of equality

$$\nabla_a \nabla_a^{\mathrm{T}} \frac{1}{\frac{1}{f} - t} = \frac{\nabla_a \nabla_a^{\mathrm{T}} f}{(1 - ft)^2} + \frac{2t}{(1 - ft)^3} \nabla_a f \nabla_a^{\mathrm{T}} f.$$

The above statements mean that adding the incompressibility terms (9) to the quasi-conformal functional (8) does not change the type of its Euler-Lagrange equations inside the feasible set. When one introduces the parameter t into (9) thus obtaining the final formulation (14) this transformation is also type-preserving inside the feasible set. Hence if the original functional which in our case is the quasi-conformal one is elliptic, then the final quasi-isometric functional is also elliptic. Moreover, the functional defined by (17) is obviously elliptic as well.

Since in the 2-D case the quasi-conformal functional coincides with the harmonic one which is well known to be elliptic the ellipticity of quasi-isometric functional is guaranteed.

2.2 Penalty formulation.

According to the success of technique from [17], instead of solving (14) with constraints (15) we suggest to solve the following problem

$$\mathbf{r}(\xi) = \lim_{\varepsilon \to \varepsilon_l,\ \varepsilon \geq \varepsilon_l} \arg\min \mathcal{I}_\varepsilon, \tag{18}$$

where

$$\mathcal{I}_\varepsilon = \int_{\mathcal{D}} (1-t) \det H \frac{\phi(A)}{\chi_\varepsilon(\det A - t\phi(A))}\, d\xi, \tag{19}$$

$$\chi_\varepsilon(q) = \frac{q}{2} + \frac{1}{2}\sqrt{\varepsilon^2 + q^2}, \quad q = \det A - t\phi(A) \tag{20}$$

and $\varepsilon_l > 0$ is sufficiently small. For the sake of brevity we will omit the argument q when writing the function $\chi_\varepsilon(q)$. Let us introduce the notations $\chi'_\varepsilon = \partial\chi_\varepsilon/\partial q$ and $\chi''_\varepsilon = \partial^2\chi_\varepsilon/\partial^2 q$. The function χ_ε possesses the following properties

$$\begin{array}{l} \chi_\varepsilon \approx q \ \text{ when } \ q \to +\infty, \quad \chi_\varepsilon \approx \frac{1}{4}\frac{\varepsilon^2}{|q|} \ \text{ when } \ q \to -\infty \\ \left|\frac{\chi'_\varepsilon q}{\chi_\varepsilon}\right| \le 1, \quad {\chi'_\varepsilon}^2 - \frac{1}{2}\chi_\varepsilon\chi''_\varepsilon \ge 0. \end{array} \tag{21}$$

The graph of $\chi_\varepsilon(q)$, $\varepsilon = 0.2$ along with its asymptotics is shown on Figure 2.

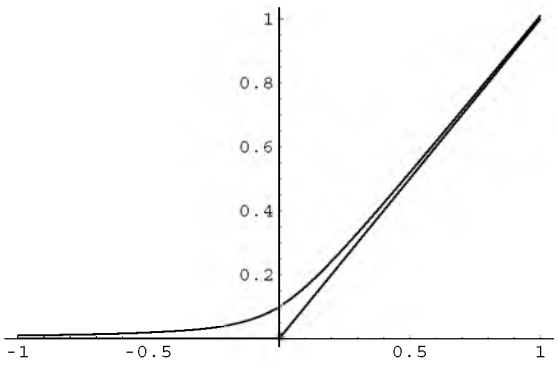

Fig. 2.

Obviously it is possible to construct other functions which look similar, however due to remarkable properties (21), this hyperbolic penalty function, suggested by I.E. Kaporin, was found to be the best regularizator for (14), (15). A similar penalty function was suggested in [26] in the context of triangular grid generation using nonlinear net of springs analogy

$$\tilde{\chi}_\varepsilon(q) = \begin{cases} q, & q > \varepsilon \\ \frac{\varepsilon^2}{2\varepsilon - q}, & q \le \varepsilon \end{cases}$$

However in [26] the variational principle was not used. For variational methods the function χ_ε is better since it is infinitely smooth and $1/\chi_\varepsilon$ is strictly convex, which is not the case for $1/\tilde{\chi}_\varepsilon$.

3 Barrier discretizations to the functional

Suppose that the valid connectivity structure of grid is defined by N_c grid cells. In the cell number c denote the vector of all cell vertices by

$$\mathbf{R}_c = \begin{pmatrix} \mathbf{X}_c^i \\ \dots \\ \mathbf{X}_c^n \end{pmatrix}, \ \mathbf{X}_c^i \in I\!R^{N_{cv}}.$$

where N_{cv} is the number of vertices in the single grid cell.

If the cell $\mathcal{D}_c$ is defined by the ordered set of N_{cv} integer numbers $v_1(c), \dots, v_{N_{cv}}(c)$, which are the pointers to the cell vertices in the total list of the grid nodes, then the following equality holds

$$\mathbf{X}_c^i = \mathcal{R}_c \mathbf{X}^i,$$

where the restriction matrix $\mathcal{R}_c \in I\!R^{N_{cv} \times N_v}$ is given by the following relations

$$\mathcal{R}_c = \{r_{ij}\}, \quad r_{ij} = \begin{cases} 1, & j = v_i(c) \\ 0, & j \neq v_i(c). \end{cases}$$

Using the above notations, the discrete counterpart of problem (14) can be formulated as follows: find the vector $\mathbf{R}$ as the solution to the following minimization problem

$$\mathbf{R} = \lim_{\varepsilon \to \varepsilon_l, \ \varepsilon \geq \varepsilon_l} \arg\min_{\mathbf{R}} \mathcal{I}_\varepsilon^h,$$

$$\mathcal{I}_\varepsilon^h = \sum_{c=1}^{N_c} \sum_{q(c)=1}^{N_q} f_\varepsilon(A)|_{q(c)} \sigma_{q(c)}, \quad f_\varepsilon(A) = (1-t) \det H \frac{\phi(A)}{\chi_\varepsilon(\det A - t\phi(A))}, \qquad (22)$$

$$\phi(A) = (1-\omega_u)\phi_c + \omega_u \phi_u, \quad \mathbf{a}_i|_{q(c)} = H_{q(c)}^{-\mathrm{T}} Q_{q(c)} \mathbf{X}_c^i, \quad \mathbf{X}_c^i = \mathcal{R}_c \mathbf{X}^i \quad ,$$

where subscript $q(c)$ denotes the $q-$th "quadrature node" for the integral over cell c, N_q matrices $Q_{q(c)}$ actually describe the discretization of the functional (19) on each element and

$$\sum_{q(c)=1}^{N_q} \sigma_{q(c)} = 1, \sigma_{q(c)} > 0.$$

It is assumed that G is constant in each cell, say,

$$G|_c = \int_{\mathcal{D}_c} G(\mathbf{r}(\xi_1, \dots, \xi_n)) d\xi,$$

however averaging in the physical space can be used as well. The feasible set $\mathcal{F}^h(t)$ is defined by $N_c N_q$ nonlinear inequalities

$$\det A - t\phi(A)|_{q(c)} > 0, \qquad (23)$$

and the discrete quasi-isometry conditions can be written as $N_c N_q$ inequalities

$$\overline{v}^{\frac{2}{n}} \gamma I \leq AGA^{\mathrm{T}}|_{q(c)} \leq \overline{v}^{\frac{2}{n}} \Gamma I,$$

where the volume factor $\overline{v}$ is defined as follows

$$\overline{v} = \sum_{c=1}^{N_c} \int_{\mathcal{D}_c} (\det G)^{\frac{1}{2}} \det S \, d\xi \, / \sum_{c=1}^{N_c} \int_{\mathcal{D}_c} \det H \, d\xi.$$

In order to account for boundary conditions we seek $\mathbf{R}$ as follows

$$\mathbf{X}^i = (I - B)\mathbf{X}_b^i + B\mathbf{X}_{in}^i, \tag{24}$$

where $B \in \mathbb{R}^{N_v \times N_v}$ is the diagonal matrix with the entries b_{ij}, such that $b_{ii} = 1$ if the i-th node of the grid is internal one, i.e., its coordinates are unknown, and $b_{ii} = 0$ when i-th grid nodes lies on the boundary and is fixed. $\mathbf{R}_b, \mathbf{R}_{in}$ are the given vector satisfying the boundary conditions, and the unknown vector, respectively.

We adopt the lexicographic local numbering scheme for each cell which is shown on Figure 3. It should be noted that for the sake of convenience the duplicate notations for the vertices of the hexahedral cell in the 3-D case are used.

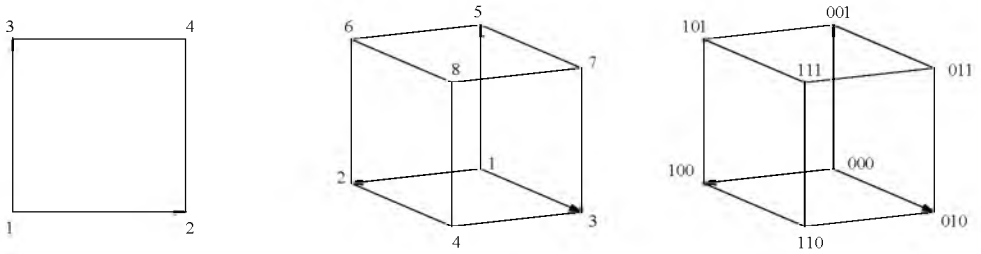

Fig. 3.

Analysis of the discrete problem (22) shows that it does not explicitly use the fact that the grid is structured, which was assumed during the derivation. It means that (22) can be used for "smoothing" of the unstructured grids, provided that the positions of the boundary nodes and the grid connectivity structure are given, i.e., the matrices $\mathcal{R}_c$ are known for each grid cell.

3.1 Barrier for quasi-isometric bilinear mapping.

The necessary and sufficient condition for the invertibility of the bilinear mapping is the convexity of the quadrilateral elements [20]. In this case the position vector $\mathbf{r}$ locally can be presented in the following form

$$\mathbf{r}(\xi_1, \xi_2) = (1 - \xi_1)(1 - \xi_2)\,\mathbf{r}(0,0) + (1 - \xi_1)\xi_2\,\mathbf{r}(0,1) + \xi_1(1 - \xi_2)\,\mathbf{r}(1,0) + \xi_1\xi_2\,\mathbf{r}(1,1),$$

and the vectors $\mathbf{a}_1, \mathbf{a}_2$ can be written as follows

$$\mathbf{a}_i = H^{-\mathrm{T}} W^{\mathrm{T}}(\xi_1, \xi_2)\mathbf{X}_c^i, \;\; W(\xi_1, \xi_2) = (\mathbf{w}_1, \mathbf{w}_2) = \begin{pmatrix} \xi_2 - 1 & 1 - \xi_2 & -\xi_2 & \xi_2 \\ \xi_1 - 1 & -\xi_1 & (1 - \xi_1) & \xi_1 \end{pmatrix}^{\mathrm{T}}.$$

Using the cell corners as the nodes of the quadrature rule we obtain that

$$Q_{2k+j+1} = W(j,k), \quad j,k \in \{0,1\}, \quad N_q = 4, \quad \sigma_i = \frac{1}{4}. \tag{25}$$

In the case $t = 0$ the resulting discrete functional has a barrier on the boundary of the set of grids with convex cells [8], while in the case $t > 0$ the barrier surrounds the set of quasi-isometric grids. It is worth noting that in the latter case the isometric condition number for interior points of each cell is bounded from above by the condition number in the cell vertices, provided that G is constant and H is constant inside each cell. This statement follows from simple observation that the value $\mathrm{tr}(A^{\mathrm{T}}A)$ in each point of bilinear cell is bounded from above by the bilinear interpolant of the values $\mathrm{tr}(A^{\mathrm{T}}A)$ computed in the cell vertices which means that inequality (15) is satisfied in each point of bilinear cell.

Other quadrature rules may result in the barrier property as well, in particular the edge centers quadratures which allow highly distorted cell shapes.

3.2 Barrier approximations for hexahedral cells.

The main requirement for discrete approximations to functional in the 3-D case is that the resulting grids should be admissible for the approximation schemes used in the solution of problems on this grids. The simplest variant here is to use the same or similar approximation schemes for the grid functional and for the governing equations of interest. Hence we will confine ourselves only to approximations which allow to compute the volume of trilinear cell exactly, i.e. which pass the simplest patch test [20]. Construction of barrier approximations to harmonic functional (5) in the 3-D case is nontrivial task [10], [16]. This is not the case for functional (14), however we will consider only such approaches which can be applied for harmonic functional as well.

Using the cell vertices $\mathbf{r}^{000}, \mathbf{r}^{100}, \mathbf{r}^{010}, \mathbf{r}^{110}, \mathbf{r}^{001}, \mathbf{r}^{101}, \mathbf{r}^{011}, \mathbf{r}^{111}$, the trilinear mapping which maps the unit cube onto the hexahedron with straight edges is written as follows

$$\begin{aligned} \mathbf{r}(\xi_1,\xi_2,\xi_3) \quad = \quad & (1-\xi_1)(1-\xi_2)(1-\xi_3)\mathbf{r}^{000} + \xi_1(1-\xi_2)(1-\xi_3)\mathbf{r}^{100} + \\ & (1-\xi_1)\xi_2(1-\xi_3)\mathbf{r}^{010} + (1-\xi_1)(1-\xi_2)\xi_3\mathbf{r}^{001} + \\ & \xi_1\xi_2(1-\xi_3)\mathbf{r}^{110} + \xi_1(1-\xi_2)\xi_3\mathbf{r}^{101} + \\ & (1-\xi_1)\xi_2\xi_3\mathbf{r}^{011} + \xi_1\xi_2\xi_3\mathbf{r}^{111}, \end{aligned} \tag{26}$$

where

$$\mathbf{r}^{ijk} = \mathbf{r}(i,j,k), \quad i,j,k \in \{0,1\}$$

which is illustrated on Figure 3.

Again using the auxiliary vectors $\mathbf{w}_i(\xi_1,\xi_2,\xi_3), i = 1,2,3$ such that

$$\mathbf{a}_i = H^{-\mathrm{T}} \begin{pmatrix} \mathbf{w}_1^{\mathrm{T}}\mathbf{X}_\zeta^i \\ \mathbf{w}_2^{\mathrm{T}}\mathbf{X}_\zeta^i \\ \mathbf{w}_3^{\mathrm{T}}\mathbf{X}_c^i \end{pmatrix},$$

we obtain from the definition of trilinear mapping (26) that

$$\begin{aligned}
\mathbf{w}_1^{\mathrm{T}} &= (-(1-\xi_2)(1-\xi_3),(1-\xi_2)(1-\xi_3),-\xi_2(1-\xi_3),\\
&\quad \xi_2(1-\xi_3),-(1-\xi_2)\xi_3,(1-\xi_2)\xi_3,-\xi_2\xi_3,\xi_2\xi_3)\\
\mathbf{w}_2^{\mathrm{T}} &= (-(1-\xi_1)(1-\xi_3),-\xi_1(1-\xi_3),(1-\xi_1)(1-\xi_3),\\
&\quad \xi_1(1-\xi_3),-(1-\xi_1)\xi_3,-\xi_1\xi_3,(1-\xi_1)\xi_3,\xi_1\xi_3) \qquad (27)\\
\mathbf{w}_3^{\mathrm{T}} &= (-(1-\xi_1)(1-\xi_2),-\xi_1(1-\xi_2),-(1-\xi_1)\xi_2,\\
&\quad -\xi_1\xi_2,(1-\xi_1)(1-\xi_2),\xi_1(1-\xi_2),(1-\xi_1)\xi_2,\xi_1\xi_2).
\end{aligned}$$

In order to obtain the matrices Q_i it is sufficient to choose the quadrature rule. In particular, the 2-point Gauss product rule with 8 quadrature nodes passes the patch test and does possess the barrier property while obviously not guaranteeing the invertibility of trilinear mapping.

3.2.1 Compound elements.

In order to construct barrier allowing only fairly good-shaped cell in relatively cheap manner let us consider the approximation based on the splitting of the grid cell into 10 auxiliary tetrahedra which are shown on Figure 4. Here 10 tetrahedra are obtained as a combination of two different conforming 5-tetrahedra splittings shown on Figures 4A and 4B, respectively.

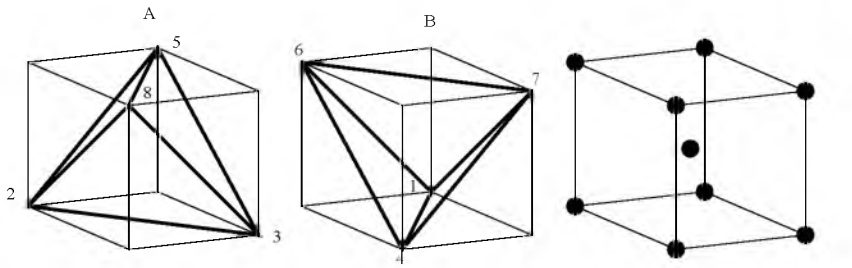

Fig. 4.

Such splittings are widely used along with the mixed finite element methods [22]. The quasi-isometry condition for hexahedron can be defined via quasi-isometry conditions for local mappings for all 10 tetrahedra. From Figure 4 it is clear that 8 tetrahedra can be assigned to the cell corners and two tetrahedra can be considered as the "central" ones. First of all we need to write down explicitly the local mappings for tetrahedra. Obviously such mappings are linear. Let us denote by $\mathbf{v}_1,\ldots,\mathbf{v}_4$ the vertices of the tetrahedron τ in the physical coordinates $\{x_1,x_2,x_3\}$ and by $\mathbf{l}_1,\ldots,\mathbf{l}_4$ the vertices of the tetrahedron T in the logical space ξ_1,ξ_2,ξ_3. The mapping $T\to\tau$

can be written via the natural coordinates resulting in the following equality

$$\begin{pmatrix} 1 \\ x_1 \\ x_2 \\ x_3 \end{pmatrix} = \begin{pmatrix} 1 & 1 & 1 & 1 \\ \mathbf{v}_1 & \mathbf{v}_2 & \mathbf{v}_3 & \mathbf{v}_4 \end{pmatrix} \begin{pmatrix} 1 & 1 & 1 & 1 \\ \mathbf{l}_1 & \mathbf{l}_2 & \mathbf{l}_3 & \mathbf{l}_4 \end{pmatrix}^{-1} \begin{pmatrix} 1 \\ \xi_1 \\ \xi_2 \\ \xi_3 \end{pmatrix}.$$

This equality allows to compute covariant basis vectors of the mapping $T \to \tau$. For corner tetrahedra these basis vectors obviously coincide with those of the trilinear mapping in the vertices of corresponding corners. It remains only to compute these vectors for "central" tetrahedra. Let us compute $\mathbf{g}_i$ for the tetrahedron shown on Figure 4B. In this case $\mathbf{v}_1 = \mathbf{r}_1, \mathbf{v}_2 = \mathbf{r}_4, \mathbf{v}_3 = \mathbf{r}_6, \mathbf{v}_4 = \mathbf{r}_7$,

$$\mathbf{l}_1 = \begin{pmatrix} 0 \\ 0 \\ 0 \end{pmatrix}, \quad \mathbf{l}_2 = \begin{pmatrix} 1 \\ 1 \\ 0 \end{pmatrix}, \quad \mathbf{l}_3 = \begin{pmatrix} 1 \\ 0 \\ 1 \end{pmatrix}, \quad \mathbf{l}_4 = \begin{pmatrix} 0 \\ 1 \\ 1 \end{pmatrix},$$

and

$$\mathbf{g}_1 = \frac{1}{2}(\mathbf{v}_2 + \mathbf{v}_3 - \mathbf{v}_1 - \mathbf{v}_4), \quad \mathbf{g}_2 = \frac{1}{2}(\mathbf{v}_2 + \mathbf{v}_4 - \mathbf{v}_1 - \mathbf{v}_3), \quad \mathbf{g}_2 = \frac{1}{2}(\mathbf{v}_3 + \mathbf{v}_4 - \mathbf{v}_1 - \mathbf{v}_2).$$

The geometrical meaning of $\mathbf{g}_i$ is obvious from Figure 4B.

The analysis for the tetrahedron shown on Figure 4A is similar. Summing up we obtain that the barrier approximation should be chosen as follows: the matrices $Q_1, \ldots, Q_8$ corresponding to the cell vertices are defined by

$$Q_{4k+2j+i} = \begin{pmatrix} \mathbf{w}_1^{\mathrm{T}}(i,j,k) \\ \mathbf{w}_2^{\mathrm{T}}(i,j,k) \\ \mathbf{w}_3^{\mathrm{T}}(i,j,k) \end{pmatrix}, \quad i,j,k \in \{0,1\},$$

while the matrices Q_9, Q_{10} corresponding to the hexahedra shown on Figure 4 can be written as follows

$$Q_9 = \frac{1}{2}\begin{pmatrix} 0 & 1 & -1 & 0 & -1 & 0 & 0 & 1 \\ 0 & -1 & 1 & 0 & -1 & 0 & 0 & 1 \\ 0 & -1 & -1 & 0 & 1 & 0 & 0 & 1 \end{pmatrix}, \; Q_{10} = \frac{1}{2}\begin{pmatrix} -1 & 0 & 0 & 1 & 0 & 1 & -1 & 0 \\ -1 & 0 & 0 & 1 & 0 & -1 & 1 & 0 \\ -1 & 0 & 0 & -1 & 0 & 1 & 1 & 0 \end{pmatrix},$$

$$N_q = 10, \sigma_1 = \ldots = \sigma_8 = \frac{1}{12}, \sigma_9 = \sigma_{10} = \frac{1}{6}.$$

These weights do guarantee that the exact volume of trilinear cell is reproduced by the approximation [27]. The above defined 10 quadrature weights and matrices Q_i fully describe the discrete approximation to the functional. It seems that such barrier is the simplest isotropic one. In principle the approximation based on only 5 tetrahedra which are shown on Figure 4A or 4B does possess the barrier property, however this approximation introduces unnecessary anisotropy into discrete functional. The above results can be applied directly in the case of tetrahedral grids and can be easily generalized for the case of prismatic cells as well.

3.2.2 Barrier allowing highly distorted cells.

The non-degeneracy of local mappings is a very restrictive condition. It arises quite naturally when using finite element methods but usually it is excessive for the finite volume methods, where the barriers can be constructed using the cell volume positivity constraint, a set of suitable cell shape constraints along with the Linear Preservation (LP) constraint which is the counterpart of the patch test for finite volume methods. In [15] it was shown that the least restrictive condition is the positiveness of the jacobian of trilinear mapping in the logical face centers, which in a sense means that the cell is not turned inside out. However the negative values of $\det S$ in the vertices and on the egdes are allowed which makes the trilinear mapping itself meaningless.

Such barrier approximation was suggested in [15]. It is illustrated on Figure 5, where two triples of the covariant basis vectors $\mathbf{g}_1, \mathbf{g}_2, \mathbf{g}_3$ from 24 possible combinations are shown. Remaining 22 triples can be obtained via rotation of the cube around logical axes.

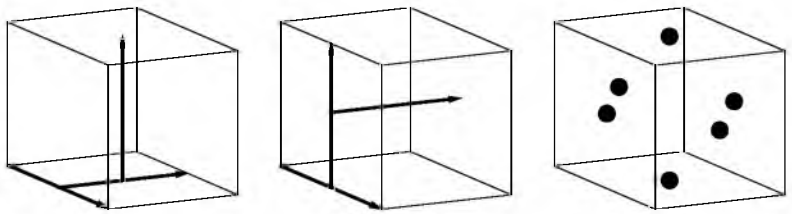

Fig. 5.

The matrices Q_1 and Q_2 corresponding to the basis vectors shown on Figure 5 look as follows

$$Q_1 = (\mathbf{w}(1/2,0,0), \mathbf{w}_2(1/2,1/2,0), \mathbf{w}_3(1/2,1/2,1/2),$$

$$Q_2 = (\mathbf{w}(1/2,0,0), \mathbf{w}_2(1/2,1/2,1/2), \mathbf{w}_3(1/2,0,1/2).$$

The matrices $Q_3, \ldots, Q_{24}$ look similar hence for the sake of brevity we will omit the explicit expressions for these matrices. The weights are defined as $\sigma_i = 1/24$.

3.2.3 Barrier for quasi-isometric trilinear mapping.

Covariant basis vectors for the trilinear mapping are defined by the following equality

$$\mathbf{g}_i(\xi_j, \xi_k) = (1-\xi_j)(1-\xi_k)\mathbf{g}_i^{00} + \xi_j(1-\xi_k)\mathbf{g}_i^{10} + (1-\xi_j)\xi_k\mathbf{g}_i^{01} + \xi_j\xi_k\mathbf{g}_i^{11}, \qquad (28)$$

where $\{i,j,k\}$ is the cyclic permutation from $\{1,2,3\}$ and

$$\begin{aligned}
\mathbf{g}_1^{mn} &= \mathbf{r}^{1mn} - \mathbf{r}^{0mn}, \quad m,n \in \{0,1\} \\
\mathbf{g}_2^{mn} &= \mathbf{r}^{m1n} - \mathbf{r}^{m0n}, \quad m,n \in \{0,1\} \\
\mathbf{g}_3^{mn} &= \mathbf{r}^{mn1} - \mathbf{r}^{mn0}, \quad m,n \in \{0,1\}
\end{aligned}$$

Using (28) we can write the jacobian of the trilinear mapping

$$J = \sum_{i,j,k,l,m,n=0}^{1} \alpha_{k+m,i+n,j+l} \mathbf{g}_1^{ij} \cdot (\mathbf{g}_2^{kl} \times \mathbf{g}_3^{mn}) \tag{29}$$

where

$$\alpha_{pqr} = \xi_1^p (1-\xi_1)^{2-p} \xi_2^q (1-\xi_2)^{2-q} \xi_3^r (1-\xi_3)^{2-r}, \quad p,q,r \in \{0,1,2\}, \tag{30}$$

and α_{pqr} are strictly positive for the interior points of the trilinear cell. It means that that if

$$\mathbf{g}_1^{ij} \cdot (\mathbf{g}_2^{kl} \times \mathbf{g}_3^{mn}) > 0, \quad i,j,k,l,m,n \in \{0,1\} \tag{31}$$

then from (29) it follows that the jacobian of the trilinear mapping is positive in the interior of the cell. Since on the boundary of cell some of the functions α_{pqr} are always positive we obtain that J will be positive on the cell boundary as well.

The total number of terms in (29) is equal to 64, however total number of different "basis functions" α_{pqr} is equal to $3^3 = 27$.

The sufficient condition of the non-degeneracy of the trilinear mapping is the positiveness of these 27 coefficients [27]. However it is not clear how to build the barrier approximation to the functional using only these 27 inequalities. Anyway, in order to compute the partial sums one needs to compute all 64 vector products, hence it is natural to consider the approximation based on $N_q = 64$. We will omit the explicit expressions for $Q_1, \ldots, Q_{64}$ and σ_i which are quite obvious while being rather cumbersome. It is not clear whether the isometric condition number of trilinear mapping is bounded from above by the maximal discrete condition number computed using all these 64 triples even when G is constant everywhere and H is constant inside each cell. Purely algebraical arguments similar to those used to characterize the feasible set make it possible to show that (15) is valid as well, i.e. local mapping inside each cell is quasi-isometric, but with smaller value t compared to that for fully discretized formulation.

It seems that simplest constructive quasi-isometry conditions for trilinear mapping are still unknown. One can expect that the barrier based on 10 tetrahedra, described in subsubsection 3.2.1 is interior with respect to trilinear mapping quasi-isometry barrier described above. It is easy to construct example of the cell where J defined by (29) is positive while the volume of one internal tetrahedron is equal to zero. The examples of the cells where all 10 tetrahedra have positive signed volumes while the trilinear mapping is degenerate are not known to the author.

3.2.4 Barriers for high order approximations.

In [15] in the case of harmonic functional it was shown that the best way to contruct barriers suitable for high order control volume methods is to do it in the hierarchical manner, by adding the constraints originating from the high order approximation schemes to the basic set of constraints associated with the conventional low order control volume methods. This is somewhat contrary to the idea of the "high order"

grid generation methods which are generally based on the bi-harmonic equations or on the high order approximations for the conventional elliptic grid generators. High order approximations should be used for grid generation with great care. In particular, in [18] it was demonstrated that finite element approximation to Winslow functional with bi-quadratic bases may result in grid folding for quite simple domains. We attribute this effect to the lack of barrier property for resulting discrete functional.

4 Example of the barrier functional behaviour for grid with one internal node

The behaviour of functional (22) can be visualized for the problem of small dimensions when the functional is the function of two variables. In [17] such analysis was done for 2-D harmonic functional and grid configuration shown on Figure 6(A). The visualization of the functional in the 3-D case is more difficult. To this end we consider the regular $3 \times 3 \times 3$ grid in the cube $-1 \leq x_i \leq 1$ with 26 fixed boundary nodes and with single free node with coordinates $\mathbf{r} = (x_1, x_2, x_3)^{\mathrm{T}}$ defined by equality

$$\mathbf{r} = \mathbf{r}_0 + \mathbf{n}_1 y_1 + \mathbf{n}_2 y_2, \quad |\mathbf{n}_i| = 1, \mathbf{n}_1^{\mathrm{T}} \mathbf{n}_2 = 0.$$

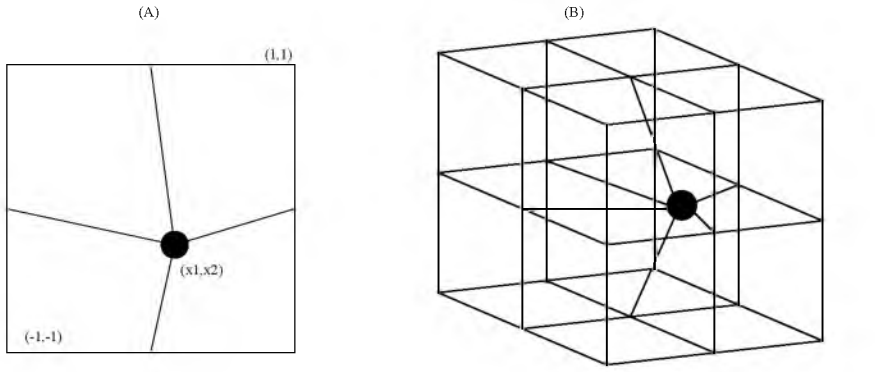

Fig. 6.

The grid configuration is shown on Figure 6(B), while the behaviour of the function $u(y_1, y_2) = \mathcal{I}_\varepsilon^h(\mathbf{r}, t)$ for compound cell approximation ($N_q = 10$) is illustrated on Figure 7. We present results for $\mathbf{n}_1 = (1, 0, 0)^{\mathrm{T}}$, $\mathbf{n}_1 = (0, 1, 0)^{\mathrm{T}}, \mathbf{r}_0 = 0$, however another choice does not lead to qualitative differences. The results in 2-D case and 3-D case are very similir.

Fig. 7.

On Figure 7, in the upper row from left to right we show the variants whith $t = 0, t = 0.7, t = 0.99$, respectively, when $\varepsilon = 10^{-9}, \omega_u = 0$. Due to the scaling along vertical axis the feasible set is clearly seen as plateau. The graphs are scaled in the horizontal plane as well since the feasible set boundary asymptotically behaves as the sphere with radius $r_d \approx 0.8\sqrt{1-t}$ which is confirmed by analysis of different cross-sections defined by the values $\mathbf{n}_1, \mathbf{n}_2$.

By construction $u(y_1, y_2)$ is an infinitely smooth function, however for small values of ε it possesses very thin transient zones which numerically should be treated as the discontinuities of the second kind. In [17] it was suggested a regularization strategy

when ε is the function of the maximal constraint violation, i.e. $\varepsilon \approx 0.2 q_{\min}$, where $q_{\min}$ is the negative value of $\det A - t\phi(A)|_{q(c)}$ with maximal module. On Figure 7, in the lower row from left to right we present the variants with $t = 0, t = 0.7, t = 0.99$, when $\omega_u = 0$ and $\varepsilon = 0.0752, 0.022, 0.0028$, respectively. The thin transient zones in this case are absent.

Similar behaviour is observed in the case $\omega_u > 0$. On Figure 8 we present the same 6 variants for $\omega_u = 0.8$. In this case the limiting feasible set boundary is the convex curvilinear multihedron with diameter $\sim \sqrt{1-t}$.

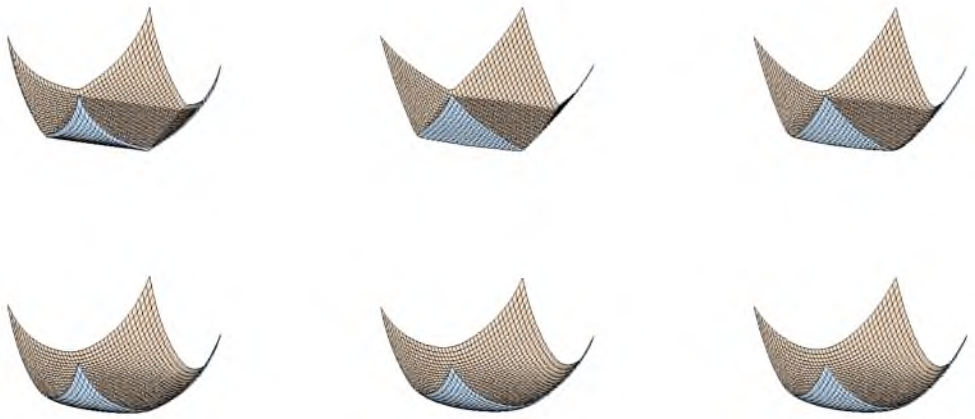

Fig. 8.

5 Minimization technique and contraction of the feasible set

In section 3 the discrete minimization problem (22) was formulated in the closed form. Similar to [17] the first step in the solution process is the grid scaling in order to have the grid coordinates of the order of unity.

The iterative solution scheme looks as follows

$$
\begin{aligned}
&\text{Choose initial guess } \; t_0 = t_b \geq 0, \mathbf{R} = \mathbf{R}^0 \\
&\text{If } \; q_{\min}(\mathbf{R}, t) < 0, \; \text{ then construct feasible solution} \\
&\text{for } k = 0, 1, 2, \ldots \\
&\qquad \text{solve approximately } \min_{\delta \mathbf{R}^k} \mathcal{I}^h_{\varepsilon_k}(\mathbf{R}^k + \delta \mathbf{R}^k, t_k) \qquad (32) \\
&\qquad \mathbf{R}^{k+1} = \mathbf{R}^k + \delta \mathbf{R}^k, \;\; t_{k+1} = \beta(\mathbf{R}^k, t_k)
\end{aligned}
$$

Here $q_{\min}(\mathbf{R}, t)$ is the minimal value of $q = \det A - t\phi(A)$ over all quadrature nodes of the grid $\mathbf{R}$, $\varepsilon_b = 10^{-9}$, and function $\beta(\mathbf{R}, t)$ is defined as follows

$$\beta(\mathbf{R}, t) = \begin{cases} (1-\delta)t_{\min}(\mathbf{R}) + \delta t_b & \text{when} \quad q_{\min}(\mathbf{R}) > 0, t_{\min}(\mathbf{R}) > t \\ t & \text{when} \quad q_{\min}(\mathbf{R}, t) > 0, t_{\min}(\mathbf{R}) \le t \\ t_{\min}(\mathbf{R}) & \text{when} \quad q_{\min}(\mathbf{R}, 0) > 0, q_{\min}(\mathbf{R}, t) \le 0 \\ t_b & \text{when} \quad q_{\min}(\mathbf{R}, 0) < 0, \end{cases} \tag{33}$$

where

$$t_{\min}(\mathbf{R}) = \min_{q(c)} \left. \frac{\det A}{\phi(A)} \right|_{q(c)},$$

and parameter $\delta = 10^{-2}$ defines the limits for contraction of feasible set.

Such complicated definition of the function $\beta(\mathbf{R}, t)$ is due to the fact that minimization problem (32) is solved approximately which can lead to bad quality or unfeasible iterates or even to reappearance of degenerate grids. In this case one should use the procedure for constructing feasible solutions anew. Suppose that the vector $\mathbf{R}^0$ is not feasible. Then this procedure can be described as follows

$$\begin{aligned} &\varepsilon_0 = \gamma(\varepsilon_b, \mathbf{R}^0) \\ &\text{for } k = 0, 1, 2, \ldots \\ &\qquad \text{solve approximately } \min_{\delta \mathbf{R}^k} \mathcal{I}^h_{\varepsilon_k}(\mathbf{R}^k + \delta \mathbf{R}^k, t) \\ &\qquad \mathbf{R}^{k+1} = \mathbf{R}^k + \delta \mathbf{R}^k, \quad \varepsilon_{k+1} = \gamma(\varepsilon_b, \mathbf{R}^{k+1}, t) \\ &\qquad \text{if } \; q_{\min}(\mathbf{R}^{k+1}, t) > 0 \;\; \text{then} \;\; \varepsilon_{k+1} = \varepsilon_b, \;\; \text{stop.} \end{aligned} \tag{34}$$

The function γ is defined as follows [17]

$$\gamma(\varepsilon, \mathbf{R}, t) = \sqrt{\varepsilon_b^2 + 0.04(\min(q_{\min}(\mathbf{R}, t), 0))^2}. \tag{35}$$

The approximate solution of the minimization problems on each step was obtained using 1-2 iterations of the gradient method with preconditioner based on the reduced Hessian matrix of $\mathcal{I}^h_{\varepsilon_k}$. Numerical experiments suggest that the procedure for constructing feasible solutions is very reliable for small values of t, while the construction of the feasible solution from the scratch for large values of t can be very difficult. Hence in numerical experiment we adopt the value $t_b = 0$, while the choice of the function β allows to expand and to contract feasible set keeping the feasibility of the current iterate. It means that we use (34) only to construct nondegenerate grids. Obviously the above described algorithm is the heuristic one, however ultimately it does contract feasible set and allows to obtain grids with small condition number. It is possible to construct a more rigorous algorithm assuming that the minimization problems with fixed t are solved exactly. However such an algorithm does not make much sense from a practical point of view and it is necessary to justify algorithms based on approximate minimization.

6 Numerical experiments

6.1 Domain with non-smooth boundary.

In the first series of numerical experiments we have considered generation of the sequence of refined grids for the domain consisting of two unit squares shifted w.r.t. each other by the vector $(3/10, -3/10)^{\mathrm{T}}$ (see Figure 9). The grid refinement results from Table 1 clearly show that harmonic grids are not quasi-isometric since their condition number grows faster than $O(N_v^{1/2})$, while the condition number of quasi-isometric grids is almost constant.

Table 1

grid size	11×21	21×41	41×81	81×161
Γ/γ	10.5	8.53	7.93	8.06
$\Gamma/\gamma\|_{\text{harmonic}}$	58.9	118.5	320.8	743.7

An examples of harmonic and quasi-isometric grids are shown on Figure 9, left and right, respectively. It is clear that large condition number of harmonic grids is due to the presence of very large and very small cells and to the grid skewness near obtuse corners.

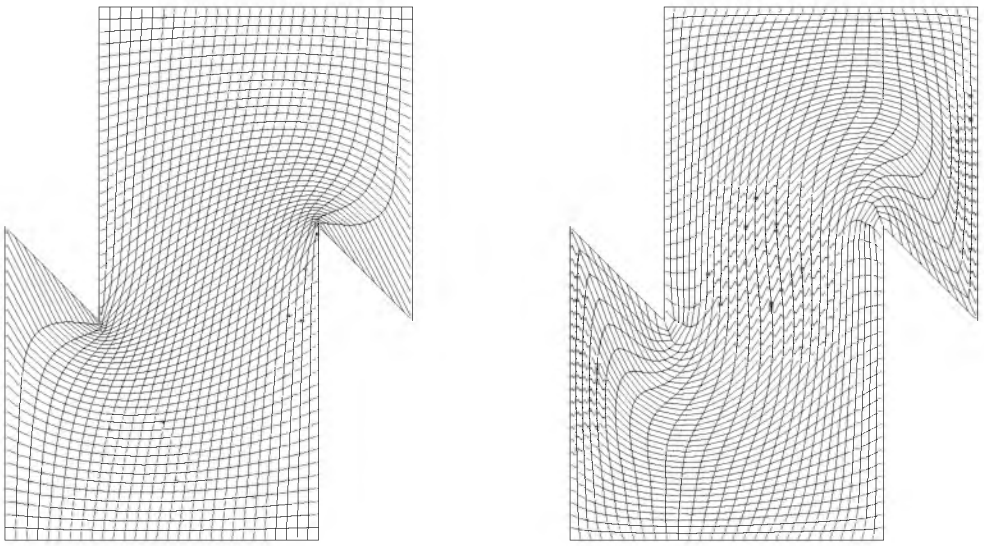

Fig. 9.

In this test case multiple solutions were not detected. Similar but more stiff problem was considered in [17] where it was shown that barrier functional possesses multiple stationary points. Numerical experiments suggest that the contraction of the feasible set by itself does not solve the non-uniqueness problem. Moreover, looking for best stationary point is senseless since all quasi-solutions are more or less close to

each other [17].

6.2 Control of grid stretching near boundary.

In the second series of tests the control of grid stretching near boundaries via accompanying metrics $H^{\mathrm{T}}H$ was investigated. The simplest case $H = H(\xi_1)$ was considered. Matrix H in each cell was obtained by computing the difference of the auxiliary mapping

$$f(\xi_1) = \xi_1 - \frac{1}{2\pi}(n_1 - 1)b \sin \frac{2\pi(\xi_1 - 1)}{n_1 - 1}, \quad 1 \le \xi_1 \le n_1, \tag{36}$$

i.e., in the cell where lower left corner has grid indices i_1, i_2,

$$h_{11} = f(i_1 + 1) - f(i_1), \quad h_{22} = 1, \quad h_{12} = h_{21} = 0.$$

The scaling coefficients should be used here since each cell in the logical space is the unit square. The grid nodes along upper and lower boundaries were distributed according to (36)

$$x_1(\xi_1) = x_1|\mathrm{corner} + (f(\xi_1) - 1)/(n_1 - 1).$$

The parameter b was chosen as $b = 0.95$ implying rather dense grids near left and right boundaries. An example of harmonic and quasi-isometric grid is presented on Figure 10, left and right, respectively.

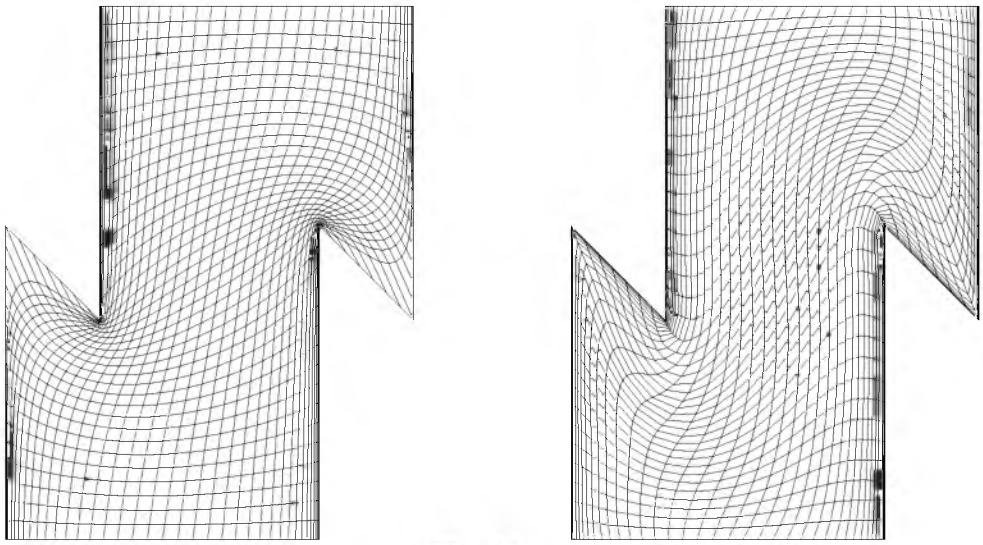

Fig. 10.

In this case the difference between two approaches is much more pronounced, which is shown in Table 2.

Table 2

grid size	11×11	21×21	41×41	81×81
Γ/γ	19.9	7.9	7.34	7.44
$\Gamma/\gamma\|_{\text{harmonic}}$	261	10^3	$2.71 \cdot 10^3$	$5.7 \cdot 10^3$

Obviously the condition number of quasi-isometric grids is almost insensitive to the grid stretching, which is not the case for harmonic grids.

6.3 Orthogonality near boundary.

In the previous example the condition numbers of quasi-isometric grids were small but these grids were not orthogonal near boundaries, since this orthogonality is not taken into account in the definition of the feasible set. In order to do this we use functional (16) with

$$\psi(H) = \overline{h}/\det H, \quad \overline{h} = \frac{1}{N_c} \sum_{c=1}^{N_c} \int_{\mathcal{D}_c} \det H \, d\xi.$$

Such choice of $\psi(H)$ means that definition of feasible set for (16) imply more stiff constraints on the shape and size of grid cells with small values of $\det H$, in particular near boundary. The effect of this modification is illustrated on Figure 11, right. This grid was obtained using $\omega_u = 0.8$ and contraction of feasible set. Its condition number is about 16.

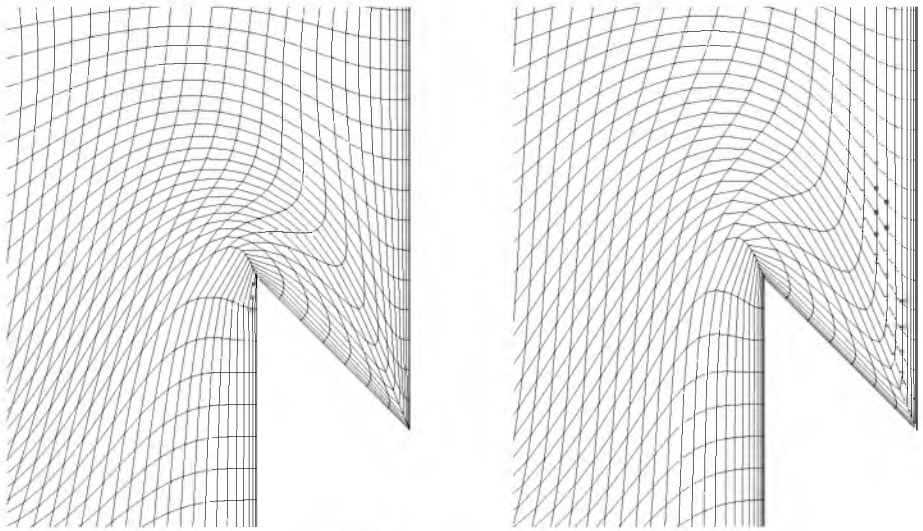

Fig. 11.

Surprisingly the "harmonic" grid which was obtained with $\omega_u = 0, t = 0$, i.e., without contraction of feasible set has very good quality as well, see Figure 11, left.

Simple modification of harmonic functional in this case results in a grid with condition number about 21, as compared to $2.71 \cdot 10^3$ in the original version. Still the quasi-isometric method provides better control over grid quality, since "harmonic" grid has step size in the normal direction to boundary 2-3 times larger as compared to that in quasi-isometric grid, which in turn precisely corresponds to the control (4).

6.4 Domain with drop-like boundary.

The domain with the drop-like boundary is one of the standard test cases for grid generators since such domains typically arise in numerical simulation of hydrodynamic instability of material interfaces. It is well known that the harmonic method in this case produces unsatisfactory results, hence one should use various additional tricks such as grid uniformity control via the constrained minimization with Lagrange multipliers [11], [18], auxiliary 1-D mapping [12], and other approaches. The comparison of harmonic and quasi-isometric grids is illustrated on Figure 12.

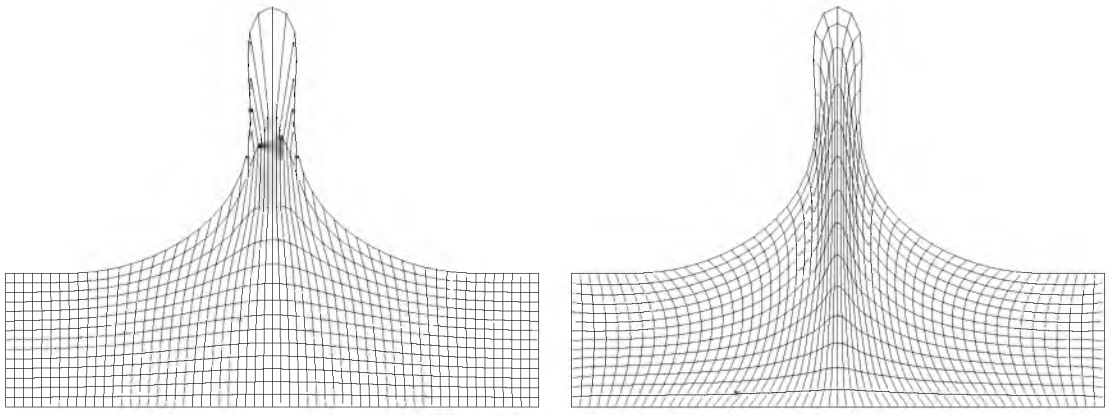

Fig. 12.

The harmonic grid is shown on the left and has the condition number 51.2, while the quasi-isometric grid is shown on the right and has condition number 15.4. The value $\omega_u = 0.95$ was used for quasi-isometric grid, however in the range of values $0.8 - 0.95$ the results are practically the same. In this example the domain boundary is smooth and it is relatively safe to use t close to unity, which generally is not recommended. On the average the best choice was $\omega_u = 0.8$.

6.5 Example of adaptive grid.

The comparison of different adaptation strategies is very complicated task largely due to problem-dependence. Hence in this paper we only consider the qualitative behaviour of several strategies. We consider the problem of grid generation in the unit square $0 < x_i < 1$ with prescribed metrics $G = G(\mathbf{r})$, where the metrics is chosen such that the grid size is smaller across the sharp gradient zones of the given function $u = u(x_1, x_2)$. For the harmonic method the metrics was chosen in such a way that the grid on the surface of the graph of the function $u(x_1, x_2)$ is as close to uniform one as possible. Then according to [6], [9]

$$G = \{g_{ij}\}, \quad g_{11} = 1 + \left(\frac{\partial u}{\partial x_1}\right)^2, \quad g_{22} = 1 + \left(\frac{\partial u}{\partial x_2}\right)^2, \quad g_{12} = \frac{\partial u}{\partial x_1}\frac{\partial u}{\partial x_2}, \tag{37}$$

while for the quasi-isometric method the following metrics was used

$$G = (1 + |\nabla u|^2)^{1/2} I. \tag{38}$$

Functional (14) can be used with both metrics, while in the harmonic one only (37) can be used. Obviously the comparison of the grid quality on the surfaces should be done using metrics (37) or even more complicated variants [6].

On Figures 13 and 14 the examples of quasi-isometric and harmonic grids, respectively, are presented. As a test function u we have chosen the function from [10] with slight modifications

$$u = \begin{cases} c & \text{if} \quad x_2 \geq y_0 + \delta \\ \frac{c}{2}(1 + \sin(\pi(q - \frac{1}{2}))) & \text{if} \quad y_0 - \delta \leq x_2 \leq y_0 + \delta \\ 0 & \text{if} \quad x_2 \leq y_0 - \delta \end{cases},$$

where

$$q = \frac{1}{2\delta}(x_2 - y_0 + \delta), \quad y_0(x_1) = 25(x_1 - \frac{1}{2})(x_1 - \frac{3}{4})(x_1 - \frac{1}{4}) + \frac{1}{2},$$

$$\delta = \delta_0 \left(1 + \left(\frac{\partial y_0}{\partial x_1}\right)^2\right)^{1/2}, \quad \delta_0 = 0.002.$$

Parameter c in two cases was different and was chosen such that the grid size across the sharp gradient zone was approximately the same for both methods. For simplicity the boundary nodes were kept fixed.

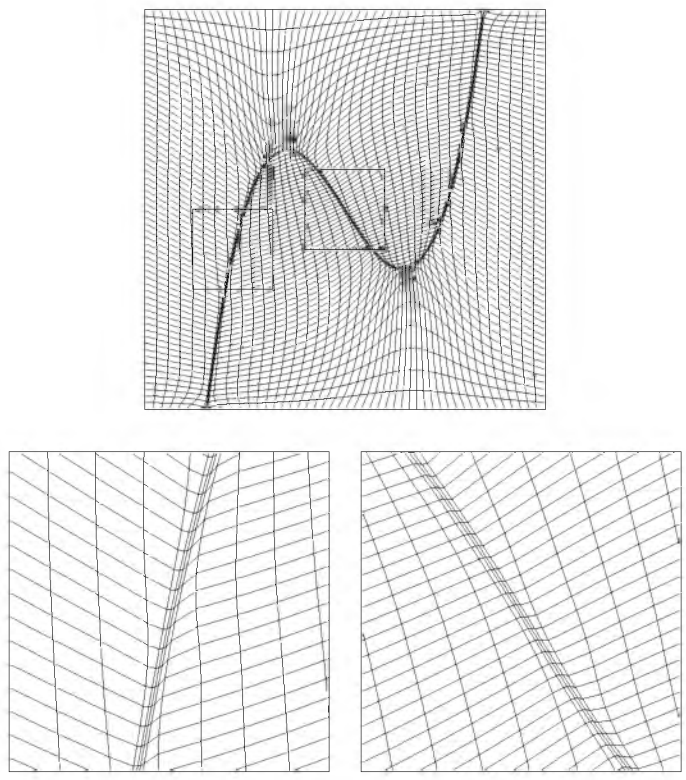

Fig. 13.

The analysis of grids shown on Figures 13, 14 suggests that harmonic grids are adapted via very skew cells in transient zones, while the cells of the quasi-isometric grids with metrics (38) are almost orthogonal in the most important part of the domain.

7 Conclusions and directions of further research

The numerical experiments allow to make the following conclusions:

- the quasi-isometric grids are smooth;
- unlike harmonic grids, the quasi-isometric grids allow to avoid very large/small grid cells near highly curved parts of the boundary;
- the skew cells and cells with large aspect ratio are absent if this is allowed by the grid connectivity and the shape of the domain;

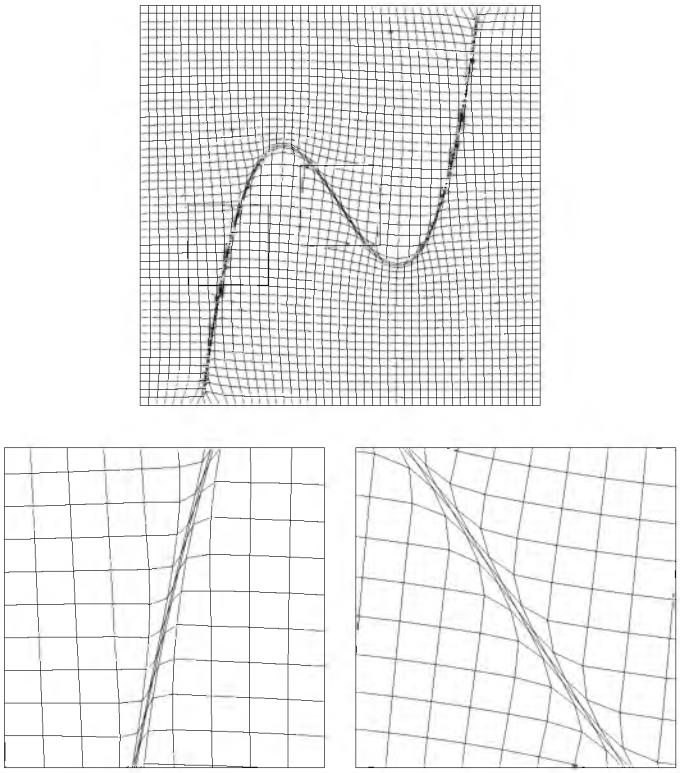

Fig. 14.

- the quasi-isometric grids can preserve orthogonality near boundary;
- with the proper choice of the control metrics $G(\mathbf{r})$ the adaptive quasi-isometric grids are almost orthogonal in the zones of sharp solution gradients.

The improvements of minimization procedure and the feasible set contraction procedure in the case when $G = G(\mathbf{r})$ are necessary. Another important problem is the development of procedures for simultaneous optimization of cell shapes and grid connectivity.

References

[1] Brackbill J.U., Saltzman J.S., Adaptive zoning for singular problems in two dimensions. J. Comput. Phys., 1982, V.46, N. 3, PP.342-368.

[2] Godunov S.K., Prokopov G.P. Calculation of conformal mappings and grid generation. Zh. Vych. Mat. Mat. Fyz., 1967, V.7, N. 6, PP.902-914.

[3] Belinsky P.P., Godunov S.K., Ivanov Yu.B., Yanenko I.K. Application of a class of quasi-conformal mappings for generation of computational grids in domains with curvilinear boundaries. Zh. Vych. Mat. Mat. Fyz., 1975, V.15, N. 6, PP.1499-1511.

[4] Dvinsky A.S. Adaptive grid generation from harmonic maps on Riemanian manifolds. J. Comput. Phys., 1991, V.95, P.450.

[5] Jacquotte O.P. A mechanical model for a new grid generation method in computational fluid dynamics. Comp. Meth. in Appl. Mech. and Eng., V.66, PP.323-338, 1988.

[6] Liseikin V.D. Construction of regular grids on n-dimensional manifolds. Zh. Vych. Mat. Mat. Fyz., 1991, V.31, N. 11, PP.1670-1683.

[7] Shepard M. and Georges M. Automatic three-dimensional mesh generation by the finite octree technique. Int. J. Num. Meth. Enrgr. 1991, V.32, PP.709-749.

[8] Ivanenko S.A., Charakch'yan A.A. Curvilinear grids consisting of convex quadrilaterals. Zh. Vych. Mat. Mat. Fyz., 1988, V.28, N.10, PP.1498-1506.

[9] Charakch'yan A.A., Ivanenko S.A. A variational form of the Winslow grid generator. J. Comput. Phys., 1997, V.136, P.385-398.

[10] Ivanenko S.A. Adaptive-harmonic grids. Comm. in appl. math., Computing Center RAS, 1997.

[11] Ivanenko S.A. Generation of curvilinear grids and their application in finite element solution of shallow water equations. Comm. in appl. math., Computing Center RAS, 1985.

[12] Charakch'yan A.A. Elliptic grid generator based on quasi-onedimensional grids. Zh. Vych. Mat. Mat. Fyz., 1999, V.39, N.5, PP.832-837.

[13] Eells J. and Sampson J. Harmonic mappings of Riemannian manifolds. Amer. J. Math., 1964, V.86, P.109-160.

[14] S.S. Antman, Regular and singular problems for large elastic deformations of tubes, wedges, and cylinders, Arch. Rational Mech. Anal, V.83, pp.1-52.

[15] Garanzha V.A., Kaporin I.E., Konshin V.N. Reliable flow solver based on the high order control volume Padé-type differences. in: Lecture Notes in Physics, Vol.515, "16th Int. Conf. on Numer. Meth. in Fluid Dyn.", Arcachon, France, 6-10 July 1998, P.278-283, Springer, 1998.

[16] Garanzha V.A., Kaporin I.E. Variational generation of grids around arbitrary trajectory wells in reservoir simulation. in: Proc. of 6 Int. Conf. on Grid Generation in CFS, Greenwich, UK, P.1001-1010, 1998.

[17] V.A. Garanzha V.A. and I.E. Kaporin, Regularization of the barrier variational grid generation method, Comp. Math. and Math. Phys., 1999, N.9.

[18] V.F. de Almeida, Domain deformation mapping: application to variational mesh generation, SIAM J. Sci. Comput., 1998, V.20, N.4, pp.1252-1275.

[19] P.G. Ciarlet, Mathematical elasticity, V.1: Three Dimensional Elasticity, Stud. Math. Appl. 20, Elsevier, New York.

[20] G. Strang, J.Fix. Analysis of finite element method. Prentice-Hall, Englewood Cliffs, NJ, 1973.

[21] Knupp P.M. Matrix norms & condition number. A general framework to improve mesh quality via node movement. in: Electronic proceedings for the 8th International Meshing Roundtable. South Lake, Tahoe, California, October 10-13, 1999. http://www.andrew.cmu.edu/user/sowen/imr8.html.

[22] Ewing R.E., Kuznetsov Yu.A., Lazarov R.D., Maliassov S. Substructuring preconditioning for finite element approximations of second order elliptic problems. I. Nonconforming linear elements for the Poisson equation in a parallelepiped, ISC research report, ISC-94-02-MATH, 1994.

[23] Kaporin I.E., On preconditioning conjugate gradient method when solving discrete counterparts of differential problems. Diff. Uravn. 1990, V.26, N.7, PP.1225-1236.

[24] Evtushenko Yu.G., Zhadan V.G, Exact auxiliary functions in optimization problems Zh. Vych. Mat. Mat. Fiz., 1990, V.30, N.1, PP.43-57.

[25] S.K. Godunov, V.M. Gordienko and G.A. Chumakov. Quasi-isometric parameterization of a curvilinear quadrangle and a metric of constant curvature, Siberian Advances in Mathematics, 1995, V.5, N.2, PP.1-20.

[26] K.Riemslaugh and J.Vierendeels, Grid generation for complex shaped moving domains, Proc. of 5th Int. Conf. on Numerical Grid Generation in Computation Field Simulation, April 1-5, 1996, Starkville, USA, pp.569-578.

[27] O.Ushakova. Personal communications.